

Ramsey fringes in a Bose-Einstein condensate between atoms and molecules

S.J.J.M.F. Kokkelmans and M.J. Holland

JILA, University of Colorado and National Institute of Standards and Technology, Boulder, Colorado 80309-0440

In a recent experiment, a Feshbach scattering resonance was exploited to observe Ramsey fringes in a ^{85}Rb Bose-Einstein condensate. The oscillation frequency corresponded to the binding energy of the molecular state. We show that the observations are remarkably consistent with predictions of a resonance field theory in which the fringes arise from oscillations between atoms and molecules.

PACS numbers: 03.75.Fi,67.60.-g,74.20.-z

Interest in the physics of ultracold molecules has been growing considerably in the past few years [1,2]. One of the goals has been the creation of a molecular Bose-Einstein condensate (BEC). In a recent experiment at JILA, performed by Donley *et al.* [3], a coherence between atoms and molecules was demonstrated in a BEC of ^{85}Rb atoms. In this experiment, two magnetic field pulses were applied to the condensate, and oscillations observed in the population of two spatially distinguishable components as a function of the pulse separation time. One of the components, the ‘remnant’ atoms, had a similar spatial profile to the original BEC. This was in contrast to a second component, the ‘burst’ atoms, which moved away from the remnant having gained a considerable amount of energy. In addition, there was a missing fraction of atoms unaccounted for after the pulse sequence. Significantly, the frequency of the population oscillations corresponded to the binding energy of the highest lying molecular state.

This observation followed other remarkable experiments carried out in the same group. The collapse of a BEC was studied when a Feshbach resonance was used to create a large negative scattering length [4]. Because of the rather violent destruction of the collapsing condensate, this effect was dubbed a ‘Bosenova’ in analogy to a supernova explosion. In a precursor experiment to the one we consider here, a single strong-coupling field pulse was applied, and there remnant and burst atoms were also observed [5].

In this letter, we describe the most recent JILA experiment by a resonance field theory that has been developed over the last two years [6–8]. This mean-field theory of dilute atomic gases goes beyond the level of the Gross-Pitaevskii equation [9,10] to include the essential pairing physics necessary to describe resonances in the two-body scattering. In the case of a Fermi gas it was applied to describe superfluidity close to a Feshbach resonance. Here, however, we are able for the first time to compare this approach with experimental data, and we obtain remarkable agreement with the observations.

A critical ingredient of the theory is the description of the Feshbach resonance. Such a resonance arises when a bound state (molecular state) lies near the threshold of the collision continuum. This bound state belongs

effectively to a channel which is energetically closed. In a system of two rubidium atoms, the position of this bound state depends on magnetic field, due to hyperfine and Zeeman interactions. The Feshbach resonance gives rise to a dispersive behavior of the scattering length, that can be formulated accurately as

$$a(B) = a_{\text{bg}} \left(1 - \frac{\Delta B}{B - B_0} \right). \quad (1)$$

Here a_{bg} is the background scattering length, ΔB the width of the resonance, and B_0 the field value where the scattering length is infinity. The magnetic field can be easily converted into an energy detuning of the molecular state from threshold by the relation $\nu_0 = (B - B_0)\Delta\mu$, where $\Delta\mu$ is the difference in magnetic moments of the energetically open and closed channels. In our theory, we treat the closed channel explicitly by using molecular field operators and ascribing a coupling to the continuum for this molecular state.

The Hamiltonian for the resonance system is given by

$$\begin{aligned} \hat{H} = & \int d^3\mathbf{x} \left(\hat{\psi}_a^\dagger(\mathbf{x})H_a(\mathbf{x})\hat{\psi}_a(\mathbf{x}) + \hat{\psi}_m^\dagger(\mathbf{x})H_m(\mathbf{x})\hat{\psi}_m(\mathbf{x}) \right) \\ & + \frac{1}{2} \int d^3\mathbf{x}_1 d^3\mathbf{x}_2 \left[\hat{\psi}_a^\dagger(\mathbf{x}_1)\hat{\psi}_a^\dagger(\mathbf{x}_2)V(\mathbf{x}_1 - \mathbf{x}_2)\hat{\psi}_a(\mathbf{x}_2)\hat{\psi}_a(\mathbf{x}_1) \right. \\ & \left. + \left(\hat{\psi}_m^\dagger\left(\frac{\mathbf{x}_1 + \mathbf{x}_2}{2}\right)g(\mathbf{x}_1 - \mathbf{x}_2)\hat{\psi}_a(\mathbf{x}_2)\hat{\psi}_a(\mathbf{x}_1) + \text{H.c.} \right) \right], \quad (2) \end{aligned}$$

where the field operators $\hat{\psi}_a^\dagger(\mathbf{x})$ and $\hat{\psi}_m^\dagger(\mathbf{x})$ create an atom or molecule at position \mathbf{x} , and H.c. denotes the Hermitian conjugate. The free Hamiltonians $H_a(\mathbf{x}) = -\hbar^2\nabla^2/2m$ and $H_m(\mathbf{x}) = -\hbar^2\nabla^2/4m + \nu$ for atoms with mass m and molecules with mass $2m$ include the detuning ν . Atom-molecule collisions and molecule-molecule collisions give higher order corrections. The potential terms $V(\mathbf{x}_1 - \mathbf{x}_2)$ and $g(\mathbf{x}_1 - \mathbf{x}_2)$ have to be chosen such that both the scattering physics and the molecular binding energies are correctly described. We verify this by noting that the scattering equations are included in this resonance mean-field theory [8]. Although unnecessary here, it is important from a fundamental perspective that the above Hamiltonian can be further generalized by the inclusion of more scattering resonances to systematically improve the description of the two-body scattering physics to any desired precision.

Starting from this Hamiltonian we obtain the Hartree-Fock-Bogoliubov (HFB) equations of motion. We define expectation values for the atomic and molecular condensates $\phi_a(\mathbf{x}) = \langle \hat{\psi}_a \rangle$ and $\phi_m(\mathbf{x}) = \langle \hat{\psi}_m \rangle$. Moreover, we define a 2×2 density matrix for the fluctuating components of the atomic field operators $\hat{\chi}_a = \hat{\psi}_a - \langle \hat{\psi}_a \rangle$, that describe the noncondensed atoms:

$$\mathcal{G}(\mathbf{x}, \mathbf{y}) = \begin{pmatrix} \langle \hat{\chi}_a^\dagger(\mathbf{y}) \hat{\chi}_a(\mathbf{x}) \rangle & \langle \hat{\chi}_a(\mathbf{y}) \hat{\chi}_a(\mathbf{x}) \rangle \\ \langle \hat{\chi}_a^\dagger(\mathbf{y}) \hat{\chi}_a^\dagger(\mathbf{x}) \rangle & \langle \hat{\chi}_a(\mathbf{y}) \hat{\chi}_a^\dagger(\mathbf{x}) \rangle \end{pmatrix}. \quad (3)$$

The elements of this matrix can be given in terms of the normal density $G_N(\mathbf{x}, \mathbf{y}) = \langle \hat{\chi}_a^\dagger(\mathbf{y}) \hat{\chi}_a(\mathbf{x}) \rangle$ and the anomalous density $G_A(\mathbf{x}, \mathbf{y}) = \langle \hat{\chi}_a(\mathbf{y}) \hat{\chi}_a(\mathbf{x}) \rangle$ [6].

To begin with, we consider a gas which is homogeneous and isotropic, which results in a translationally invariant system. This implies that the single particle fields are constant in space, and that the two-particle fields depend on the coordinate difference $r = |\mathbf{x} - \mathbf{y}|$ only. We substitute local interactions for the potential terms: $V(r) = V\delta(r)$ and $g(r) = g\delta(r)$, where V and g are constants. The HFB equations for the density matrix \mathcal{G} and for the condensate fields ϕ_a and ϕ_m are obtained from the Heisenberg equations for the field operators, having taken expectation values and applied Wick's theorem:

$$i\hbar \frac{d\phi_a}{dt} = V(|\phi_a|^2 + 2G_N(0))\phi_a + (VG_A(0) + g\phi_m)\phi_a^*, \quad (4)$$

$$i\hbar \frac{d\phi_m}{dt} = \frac{g}{2}(\phi_a^2 + G_A(0)) + \nu\phi_m, \quad (5)$$

$$i\hbar \frac{dG_N(r)}{dt} = 2\text{Re} [V(\phi_a^2 + G_A(0))G_A^*(r) + g\phi_m G_A^*(r)], \quad (6)$$

$$i\hbar \frac{dG_A(r)}{dt} = -\frac{\hbar^2 \nabla^2}{2\mu} G_A(r) + 4V(|\phi_a|^2 + G_N(0))G_A(r) + [V(\phi_a^2 + G_A(0)) + g\phi_m](2G_N(r) + \delta(r)), \quad (7)$$

with μ the reduced mass. This is the complete closed set of equations to be dynamically solved. As emphasized earlier, the binary collision physics encapsulated in the HFB equations is extracted by setting the density dependent shifts to zero

$$i\hbar \frac{d}{dt} \mathcal{P}(r) = \left[-\frac{\hbar^2 \nabla^2}{2\mu} + V\delta(r) \right] \mathcal{P}(r) + g\delta(r)\phi_m, \quad (8)$$

$$i\hbar \frac{d}{dt} \phi_m = \frac{g}{2} \mathcal{P}(0) + \nu\phi_m, \quad (9)$$

where $\mathcal{P}(r) = \phi_a^2 + G_A(r)$ is the total pairing field, leaving the two coupled two-body scattering equations with contact interactions [8].

The local potentials in Eqns. (4)-(7) give rise to an ultraviolet divergence, which can be properly treated by renormalization. This must be done in such a way as to maintain the correct underlying two-body resonance physics for any momentum cutoff K in the field theory. One should consider the delta function interactions

to be appropriate zero range limits of nonlocal potentials (e.g. square well potentials), and the properties of these potentials can then be chosen such that the microscopic low energy two-body physics around a Feshbach resonance is correctly described. This renormalization procedure amounts to replacing the coupling constants in the Hamiltonian by parameters which depend on K . The required parameters can be concisely summarized by the complete relations $V = \Gamma U$, $g = \Gamma g_0$, and $\nu = \nu_0 + \alpha g g_0 / 2$, where $U = 4\pi\hbar^2 a_{\text{bg}} / m$, $\Gamma = (1 - \alpha U)^{-1}$, $\alpha = mK / (2\pi^2 \hbar^2)$, and g_0 is determined from the field dependence of the binding energy as we now explain.

A big advantage for this system is that the rubidium two-body interactions are extremely well known. Typical scattering lengths can be calculated to at least the 1% level [11]. For this experiment, where the fringe frequency is determined by the energy of the highest bound state, accurate knowledge of the binding energy is crucial. In Fig. 1 we show the binding energy as a function of magnetic field using a full coupled channels calculation [12]. This calculation consists of all relevant rubidium two-body interactions including hyperfine and Zeeman interactions and electron-spin dependent singlet and triplet potentials. In order to reproduce exactly the result of the full coupled-channels calculation, we would need to go beyond the single resonance formulation we have presented. However, in spite of the complexity of the real rubidium system, the field theory with one resonance state allows a remarkably good approximation to the binding energy over the field range of interest. This comparison is shown in Fig. 1 and determines the value of g_0 used in our following simulations.

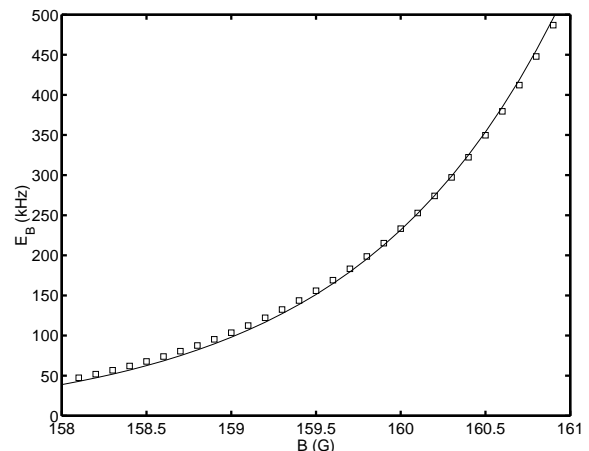


FIG. 1. Binding energies as a function of magnetic field. The solid line is the coupled channels result for the most accurate rubidium interactions. This is compared with the binding energy resulting from a contact scattering model with $a_{\text{bg}} = -450a_0$ (where a_0 is the Bohr radius), $\Delta\mu = 2.23\mu_B$ (with μ_B the Bohr magneton), and $g_0 = 3.11 \times 10^{-38} \text{ Jm}^{3/2}$ (open squares).

The outcome of the experiment of Donley *et al.* [3]

closely resembles the seminal experiments on Ramsey fringes in atomic beam physics [13]. The starting point is a condensate of ^{85}Rb atoms in the $|f, m_f\rangle = |2, -2\rangle$ state, at a magnetic field where the scattering length is close to zero. Two magnetic field pulses are applied (a schematic is shown in Fig. 2), each of which brings the condensate close to resonance. The two pulses are separated by a free evolution interval t_{evolve} , during which time the magnetic field is increased to move the system further away from resonance. After this pulse sequence, the remaining number of atoms in the condensate is measured, which is then called the remnant. Also a burst of noncondensate atoms is observed. The populations of the remnant and burst both show oscillations as function of t_{evolve} at a frequency that corresponds to the binding energy of the molecular state at the intermediate field. The sum of the populations of the remnant and burst do not add up to the initial number, implying a missing component. The theoretical solutions which follow in this Letter can be directly compared with the results presented in the figures of Donley *et al.* [3].

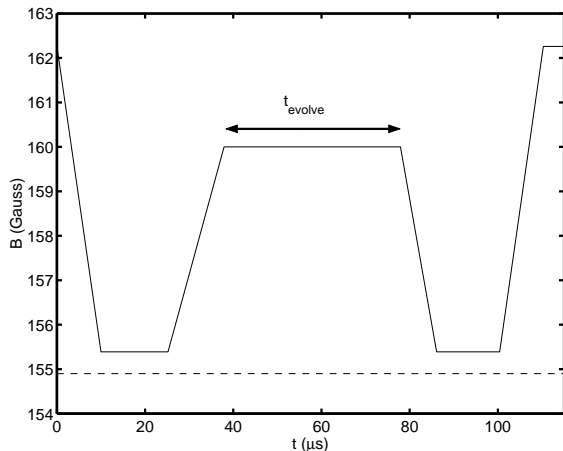


FIG. 2. A typical magnetic field pulse sequence as a function of time. The interval t_{evolve} is modified in the experiment. The position of the resonance is indicated by the dashed line.

In spite of the fact that the mean-field Eqns. (4)-(7) were derived for a homogeneous system, we may apply our theory to a trapped gas. At the highest energy scales reached during the evolution, the velocity of the atoms is sufficient to move only one hundredth of the oscillator ground state size in the tightest direction during the full evolution time. Therefore, a complete quantum description of the oscillator levels is not required. Instead, we use a local density approximation and perform a Gaussian average over the densities of the gas. For each value of the density, we solve the time-dependent equations modifying the detuning according to the time-dependent field given in Fig. 2. In Fig. 3 we show a time evolution of the atomic condensate, and the corresponding time evolution of the molecular condensate. At the end of the

first pulse about 25% of the condensate atoms have been converted into other components. The growth of population in the molecular condensate takes place mostly during the final ramp. It is notable that the fraction of molecules does not account for the missing atoms. In fact, the atoms are mainly transferred to the normal and anomalous densities which are ascribed to the noncondensate component.

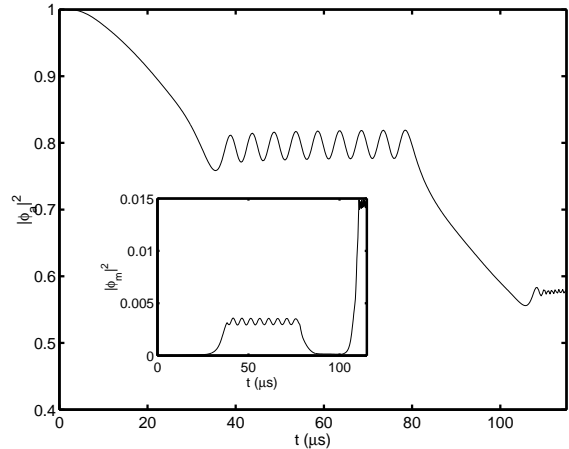


FIG. 3. Fraction of the atomic condensate as a function of time. We identify these atoms as the remnant of Donley *et al.* [3]. The calculation is done for the pulse sequence given in Fig. 2, for a density $n = 3.9 \times 10^{12} \text{ cm}^{-3}$. The inset shows the analogous graph for the molecular condensate.

The growth of the noncondensate component can be seen in Fig. 4. The function $G_N(r=0)$ represents the density of noncondensate atoms, which can be seen to oscillate out of phase with the atomic condensate during t_{evolve} . It is remarkable that in spite of the fact that the Ramsey fringes occur at the molecular binding energy with significant visibility, the population of the molecular condensate remains small. A much larger fraction is converted into strongly correlated atom pairs, encapsulated by the normal and anomalous densities. Interestingly, the anomalous density is the same aspect of the field theory which accounts for Cooper pairing in a nonideal Fermi gas and gives rise to superfluidity at temperatures below the critical value. The explanation for the observed growth of the pairing field rather than the molecular condensate is due to the close proximity of the bound state to threshold. The range of the molecular bound state stretches in this case to very large internuclear distances, something which has much more overlap with the delocalized G_A pairing field than with the localized closed channel state.

In Fig. 5 we show the population of atomic condensate and noncondensate atoms, obtained at the end of the pulse sequence, as a function of the evolution time t_{evolve} . The sum of these two numbers (squares) equals the total number of initial condensate atoms minus twice

the number of molecular condensate atoms due to particle conservation. The frequency of the oscillations agrees with the binding energy of the renormalized potential, given by the open squares in Fig. 1. When we compare these curves with Fig. 5 of Donley *et al.* [3], we see that we can clearly identify the remnant observed in the experiment as the atomic condensate component of the quantum field theory. The experimental data closely resembles the solid curve both in offset and in amplitude. Similarly, the noncondensate atoms can be identified as the burst atoms. Since $G_N(r)$ is a correlation function, it is straightforward to determine the energy of the noncondensate atoms which are produced. This manifests as the spatial decay rate of the correlation function in the r -direction, which can be converted into an average energy. The energy which results is comparable to the experimentally determined energy range for the burst. The missing atoms are also elucidated. Note that there is a large time interval between the final ramp and the time at which the atomic absorption imaging takes place. These weakly bound molecules may decay to lower vibrational states via a collision with a third atom, resulting in large kinetic energies for both scattering partners. Such atoms would not be observed.

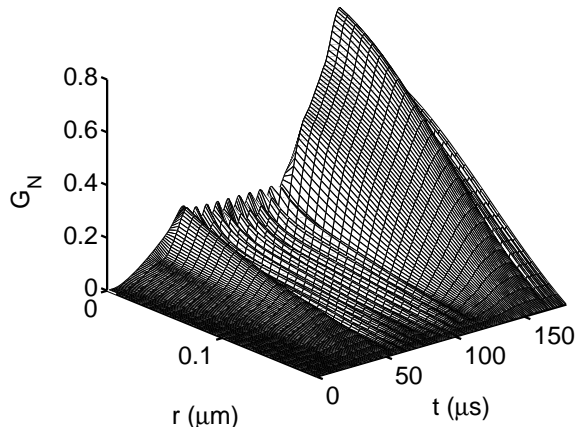


FIG. 4. Normal field $G_N(r)$ as a function of time and distance for the same calculation illustrated in Fig. 3. We identify these atoms as the burst atoms of Donley *et al.* [3]. The spread in r -space is a measure of the energy of these noncondensate atoms.

We have repeated our calculation for a different experimental situation [14] with a factor 10 larger density, and a different time-dependence of the field. Here the number of remnant atoms is lower than the burst atoms, so that the position of the fringes shown in Fig. 5 are switched and show indications of damping. We again get good agreement with the experiment, and the appearance of damping of the Ramsey fringes in the theory is due to density-dependent inhomogeneous dephasing. This effect is due to a relatively small shift in the oscillation

frequency that shows a strong dependence on density. Finally we note that both theory and experimental data exhibit a notable phase-shift between the position of the fringes of the atomic condensate and the noncondensate atoms.

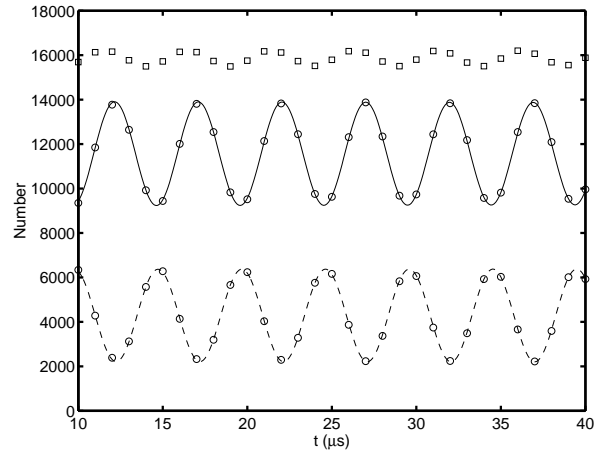


FIG. 5. Oscillations between the atomic condensate (solid line) and the normal field $G_N(0)$ (dashed line). These two numbers add up to the total number of recovered atoms (squares), which excludes the molecular component. The calculation is performed for a mean density of $\langle n \rangle = 3.9 \times 10^{12} \text{ cm}^{-3}$. This case can be directly compared with Fig. 6 of Donley *et al.* [3].

In conclusion, we have used a resonance effective field theory which includes an accurate description of the two-body bound state and scattering physics to describe a recent experiment at JILA. Because of the complexity of the mean-field physics relevant to Feshbach resonance scattering, it has not been possible previously to provide this kind of quantitative comparison. We are able to unambiguously identify the observed remnant and burst. The pairing field associated with the noncondensate atoms plays a crucial role in our calculated evolution. This pairing field is analogous to the formation of Cooper pairs in a superfluid Fermi gas. The ability to determine the coupling constants from known two-body rubidium physics allows us to make these comparisons with experimental data with no adjustable parameters.

We thank J. Cooper, J. Milstein, E. Donley, N. Claussen, S. Thompson, E. Cornell and C. Wieman, for stimulating discussions. Support is acknowledged for S.K. from the U.S. Department of Energy, Office of Basic Energy Sciences via the Chemical Sciences, Geosciences and Biosciences Division, and for M.H. from the National Science Foundation.

- [1] R.H. Wynar, R.S. Freeland, D.J. Han, C. Ryu, and D.J. Heinzen, *Science* **287**, 1016 (2000).
- [2] D.J. Heinzen, R. Wynar, P.D. Drummond, and K.V. Kheruntsyan, *Phys. Rev. Lett.* **84**, 5029 (2000).
- [3] E.A. Donley, N.R. Claussen, S.T. Thompson, and C.E. Wieman, cond-mat/0204436.
- [4] E. A. Donley, N. R. Claussen, S. L. Cornish, J. L. Roberts, E. A. Cornell and C. E. Wieman, *Nature* **412**, 295 (2001).
- [5] N.R. Claussen, E.A. Donley, S.T. Thompson, C.E. Wieman, cond-mat/0201400.
- [6] M. Holland, J. Park, and R. Walser, *Phys. Rev. Lett.* **86**, 1915 (2001).
- [7] M. Holland, S.J.J.M.F. Kokkelmans, M.L. Chiofalo, and R. Walser, *Phys. Rev. Lett.* **87**, 120406 (2001).
- [8] S.J.J.M.F. Kokkelmans, J.N. Milstein, M.L. Chiofalo, R. Walser, and M.J. Holland, accepted for publication in *Phys. Rev. A.*, cond-mat/0112283.
- [9] E. Timmermans, P. Tommasini, R. Ct, M. Hussein, and A. Kerman, *Phys. Rev. Lett.* **83**, 2691 (1999).
- [10] M. Mackie, R. Kowalski, and J. Javanainen, *Phys. Rev. Lett.* **84**, 3803 (2000).
- [11] E.G.M. van Kempen, S.J.J.M.F. Kokkelmans, D.J. Heinzen, and B.J. Verhaar, *Phys. Rev. Lett.* **88**, 093201 (2002).
- [12] The coupled channels binding energy has been obtained by using the most accurate rubidium two-body interactions to date [11].
- [13] N.F. Ramsey, *Rev. Mod. Phys.* **62**, 541 (1990).
- [14] Donley *et al.*, priv. comm.